

ARTICLES

Time-Resolved Photodissociation Rates and Kinetic Modeling for Unimolecular Dissociations of Iodotoluene Ions

Chuan Yuan Lin and Robert C. Dunbar*

Chemistry Department, Case Western Reserve University, Cleveland, Ohio 44106

Received: October 13, 1993*

Time-resolved photodissociation rate measurements are reported for the unimolecular dissociation of the three iodotoluene ion isomers at two values of internal energy (2.54 and 2.67 eV). For the para isomer, the rate constants are in agreement with previous experimental information. The meta isomer is roughly similar to para, but the ortho isomer dissociates roughly 5 times faster at the same internal energies. These new data, along with prior results, are fitted into a comprehensive two-channel model of the dissociation kinetics, assuming competitive dissociation to form tolyl ions, and either benzyl or tropylium ions. Activation energies and entropies are assigned to both dissociation channels for each isomer. This two-channel model accounts satisfactorily for most of the experimental information available about these dissociation processes, and possible explanations are advanced to explain discrepant data.

Introduction

The fragmentation of iodotoluene ions is a historically intriguing, kinetically complex situation whose general features are rapidly being clarified by new, powerful techniques for studying unimolecular dissociation kinetics. This system presents an interesting kinetic and mechanistic contrast to iodobenzene ions. The latter undergo a simple bond-cleavage dissociation, involving a loose transition state, yielding phenyl cation and an iodine atom.¹ Iodotoluene shows a similar cleavage of the iodine atom, but the mechanism, the nature of the transition states, and the structure of the product ions reflect more complex events than simple bond cleavage. The complexity of the mechanism has led to a long series of experimental studies using increasingly powerful techniques.²⁻⁹ The iodotoluene system is quite clearly a classic example of (at least) two distinct, competing pathways to products having the same stoichiometry, with the extent of

competition depending in an interesting way on the internal energy of the ion and also on which of the three parent-ion isomers is used.

Along with adding new kinetic data to the existing picture, the present study attempts a more complete synthesis of the existing data into a coherent overall picture than has been achieved in previous work. There is enough now known about these dissociations that it seems worth attempting a quantitative understanding of the kinetics. We have undertaken a critical examination of the available kinetic and mechanistic data, with the goal of putting together a global kinetic model for all three isomers.

The two-channel picture widely accepted for these dissociations can be formulated as follows. Parent ions having enough excess internal energy to dissociate can do so through either of two competing reaction channels. We will assume that the branching between the two channels, and the rates of dissociation, depend only on the internal energy of the ion and can be calculated using the RRKM (Rice-Ramsperger-Kassel-Marcus) formulation of

* To whom correspondence should be addressed.

• Abstract published in *Advance ACS Abstracts*, January 1, 1994.

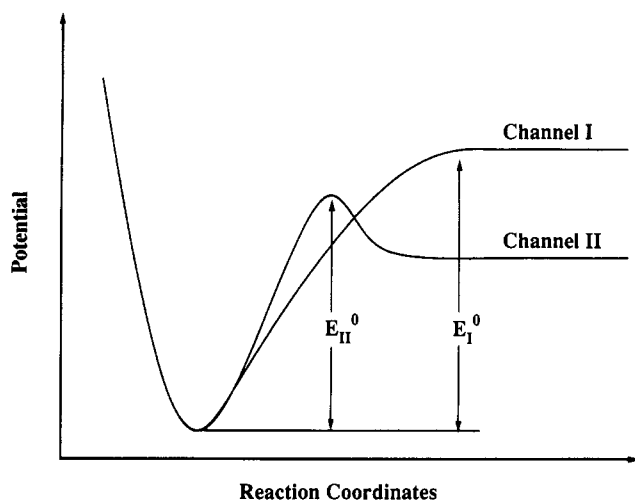
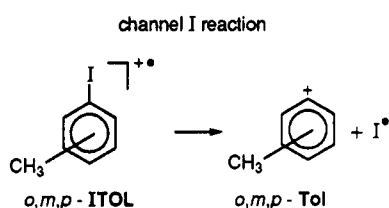
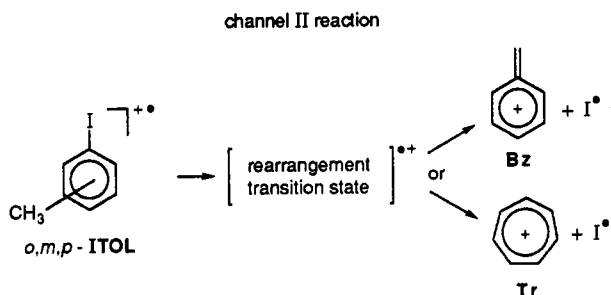


Figure 1. Schematic diagram of the postulated potential curves for the two-channel model of iodotoluene ion dissociations.

transition state theory.¹⁰ The direct cleavage pathway, which we will call channel I, cleaves the C–I bond to give tolyl ion (Tol):



The rearrangement pathway, which we will call channel II, involves some sequence of rearrangements of the parent ion structure yielding either tropylium ion (Tr) or benzyl ion (Bz). The nature of these rearrangements, and the identity of the channel II product ion, are largely matters of speculation at this point.



The activation energy and entropy for channel II are determined by a transition state lying much higher in energy than either the tropylium or benzyl products, so that the kinetics of channel II bear no relation to the overall thermochemistry of the dissociation. It is this complete decoupling of the properties of the channel II transition state and the reaction products which has frustrated attempts to draw thermochemical implications from the threshold behavior of iodotoluene ion dissociations. Figure 1 presents a schematic picture of the potential energy curves for this two-channel model.

The new kinetic data described here were measured by the technique of time-resolved photodissociation (TRPD) in the ion cyclotron resonance (ICR) ion trap.¹¹ This technique exploits the precise energy control inherent in photoexcitation, along with careful thermalization of the ions, to measure dissociation rates for ions of well-characterized energies.

Because of limitations of available laser wavelengths and also limitations imposed by the spectroscopic absorptions of the ions, TRPD studies typically have given dissociation rates at only a few internal energies. However, the data points obtained from

this technique are often extraordinarily valuable, because they represent unambiguous rate values for ions of confidently known internal energy. Of the approaches widely employed to measure dissociation kinetics, only the photoelectron photoion coincidence (PEPICO) technique¹² shares this characteristic; these two techniques are complementary, with PEPICO being most widely used for fast dissociations and TRPD for slow ones.

Experimental Section

The time-resolved photodissociation (TRPD) experiments were carried out on an ion cyclotron resonance (ICR) mass spectrometer equipped with phase-sensitive detection and were similar to the *p*-ITOL experiments described in ref 3. Ions formed by electron impact from iodotoluene vapor were trapped in the ICR ion trap for several seconds. Dissociation was initiated by a 10-ns laser pulse; the subsequent dissociation into fragments was followed as a function of delay time after the laser pulse.

Ionization was by an electron beam pulse of about 100-ms duration at a nominal electron energy of 8–10 eV. A 2.5-V dc voltage was applied on the two trapping plates to trap the ions in the 2.5-cm cubical cell. The operating pressure was $(3\text{--}4) \times 10^{-7}$ Torr of iodotoluene giving about 10 ion-neutral collisions/s. Before being irradiated with the laser pulse, parent ions were allowed to thermalize for at least 2.5 s. This is expected to be ample time for removal of any superthermal internal energy by collision with parent neutrals and by radiative cooling. Photo-product detection was achieved by applying an excite pulse of 20- μ s duration with 50-V peak-to-peak amplitude at the frequency of $C_7H_7^+$, followed by a 3-ms ICR transient acquisition. The experimental sequence and data acquisition were automated under microcomputer control. The magnetic field was 1.4 T. A data acquisition mode using alternating light-on/light-off cycles was used to give baseline stabilization and to subtract out the signal contribution from $C_7H_7^+$ ions produced by electron impact.

Two wavelengths were used in this work. At 532 nm the laser pulse was the doubled output of Lumonics HY 1200 Nd:YAG laser. The 504-nm laser pulse was generated using 355 nm from the tripled YAG fundamental to pump the Lumonics Hyperdye 300 dye laser with C500 laser dye. Laser pulses were of the order of 3–10 mJ.

Results

Time-resolved photodissociation data were taken at two wavelengths for each isomer, as displayed in Figure 2. Each time-resolved series was accumulated for at least 100 scans. As was described previously for *p*-ITOL³ there was a nonzero intercept at zero delay time for all three isomers. This phenomenon was attributed to two-photon dissociation, which is expected to involve ions dissociating very fast on the time scale of these experiments and thus to give a nonzero daughter-ion intensity at zero delay time.

At these two wavelengths, the total internal energies (the energy of one photon plus thermal energy at 375 K) were not far above the dissociation thresholds, giving slow rate constants for fragment ion appearance ranging from 1.1×10^3 to 3.5×10^4 s⁻¹. Assuming that the IR-radiative characteristics of the three isomers are similar, we can use the previous *p*-ITOL results³ to estimate the contribution made by the radiative relaxation process to the apparent parent-ion disappearance rate constants. The radiative relaxation value of 160 s⁻¹ assigned to *p*-ITOL is almost an order of magnitude slower than the slowest rate measured here, so that the radiative relaxation correction is in any case small and need not be made with high accuracy. A radiative relaxation rate of 160 s⁻¹ was assumed in fitting all the data.

The fitting of TRPD data to include the effects of the ICR-TRPD signal equation,¹³ the rate energy curve, the thermal spread of ion energies, and the radiative relaxation process was carried out as in ref 3. Sample TRPD data and the corresponding fits

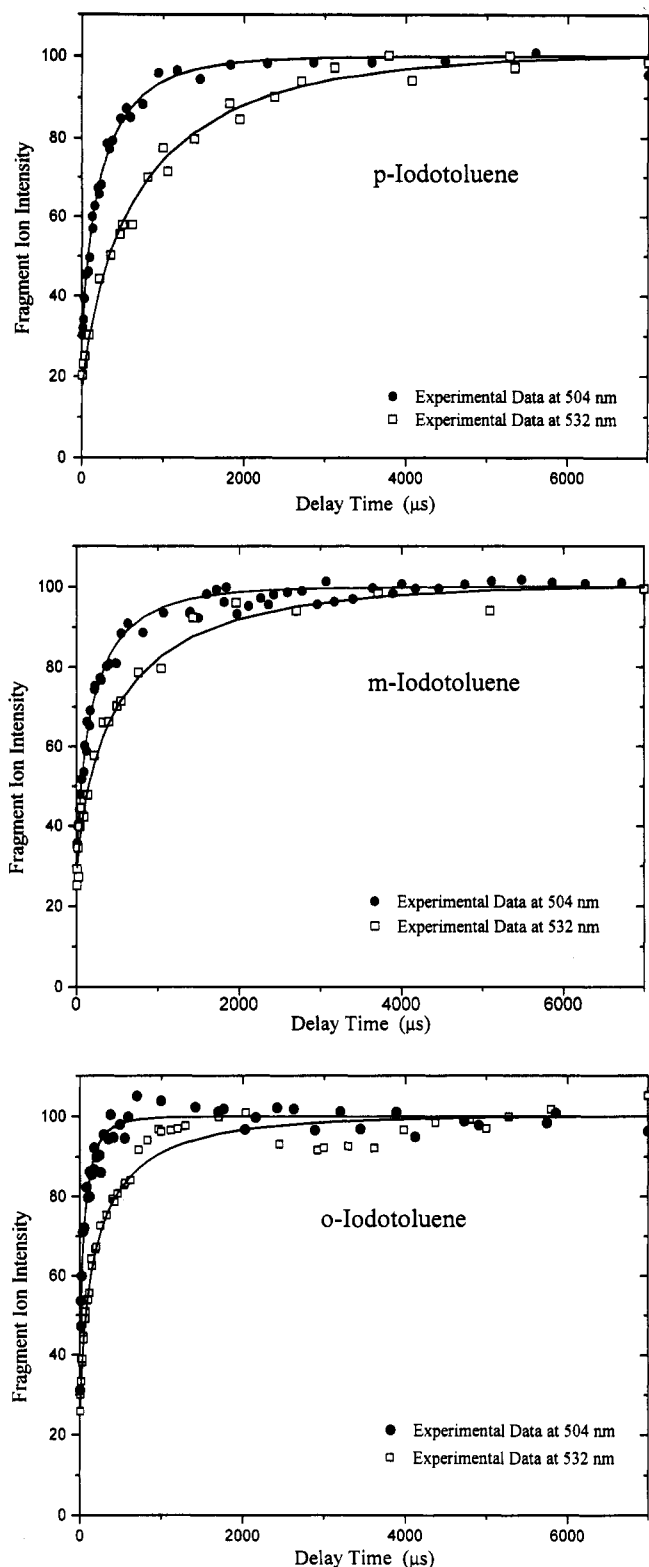


Figure 2. TRPD data plots for the three iodotoluene ions at 504 and 532 nm. The solid curves represent the modeled curves according to the present two-channel picture, using the activation parameters listed in Table 3.

are displayed in Figure 2. The solid curves shown with the data are the calculated curves corresponding to the rate-energy curves given below for the three isomers (Figure 7 below), and the fit to the data is seen to be good in all cases. The dissociation rate constants derived from the fits are given in Table 1. One striking aspect of the results is that while para and meta show comparable dissociation kinetics, the ortho isomer dissociates about 5 times faster at similar internal energies. Clearly one key goal of interpretation and modeling is to account for this large difference.

TABLE 1: Dissociation Rate Constants (s^{-1})

photodissociation wavelength (nm)	av internal energy (eV)	para	meta	ortho
504	2.67	4167	5607	35450
532	2.54	1150	1775	7356

TABLE 2: Literature Heats of Formation

species	heat of formation (kJ mol^{-1} at 0 K)
C_7H_7^+ (Tr)	888 ^a 872 ^b
C_7H_7^+ (<i>o</i> -Tol)	(no value)
C_7H_7^+ (<i>m</i> -Tol)	1079 ^c
C_7H_7^+ (<i>p</i> -Tol)	1096 ^c
C_7H_7^+ (Bz)	919 ^d
$-\text{C}_6\text{H}_4\text{CH}_3\text{I}^{+\bullet}$ (<i>p</i> -ITOL)	958 ^b
$-\text{C}_6\text{H}_4\text{CH}_3\text{I}^{+\bullet}$ (<i>m</i> -ITOL)	982 ^b
$-\text{C}_6\text{H}_4\text{CH}_3\text{I}^{+\bullet}$ (<i>o</i> -ITOL)	982 ^b
I	107.2 ^b

^a Reference 5, corrected to 0 K by adding 23 kJ mol^{-1} . ^b Reference 16. ^c References 14 and 15. ^d Reference 14.

Thermochemistry

The important sources of reliable quantitative thermochemistry relevant to these systems (Table 2) are the following: The heats of formation of the parent ions are known reliably from photoionization. *p*- and *m*-Tol isomers were assigned by Baer et al. from nitrotoluene dissociations,¹⁴ with uncertainties of 10 kJ mol^{-1} ; their values were slightly adjusted by the reanalysis of Klots.¹⁵ There is a good consensus on the heat of formation of benzyl ion, near the values shown in the table. The tropylium ion is more uncertain: the first value given in the table is a recent measurement (corrected to 0 K) supported by a reasonable ab initio calculation,⁵ while the second is the critically evaluated value from Lias et al.¹⁶ In our opinion, none of these Tr, Bz, or Tol heats of formation are currently known with unshakeable confidence to within ± 15 kJ mol^{-1} , because all of the experiments have troubling uncertainties about the isomeric nature of the observed ions, while no theoretical calculations at a convincingly high level of precision have been reported.

Kinetic Scheme and Modeling

Recent thinking about these systems has been based on the straightforward two-channel scheme, in which the iodotoluene ion dissociates competitively into tolyl ions (channel I) and tropylium and/or benzyl ions (channel II). In our present effort to give a satisfactory overall understanding of these ions, we have fitted all of the reliable experimental information about these systems into this scheme, although the rate constants, kinetic parameters, and branching ratios that we derive here are not similar to those used in previous analyses.

There were four variables in this fitting: $\Delta S_{\text{I}}^{\ddagger}$, $\Delta S_{\text{II}}^{\ddagger}$, E_0^{I} , and E_0^{II} , where ΔS^{\ddagger} is the entropy of activation at 1000 K, and E_0 is the activation energy. The definition and use of these kinetic parameters to describe ionic dissociations within the framework of RRKM theory has been discussed.¹⁷

Several features were considered desirable in constructing the kinetic models and were incorporated in our kinetic model: (1) Channel I should have a loose transition state, reflected in a strongly positive activation entropy. (2) Channel II should have a tight transition state, reflected in a near-zero or negative activation entropy. (3) The channel I activation entropies and energies should be close to those previously established for iodine cleavage in iodobenzene ion. However, since the fit of the models to experiment was extremely sensitive to the channel I activation energy, the E_0^{I} values for channel I were allowed to differ by small amounts between the isomers. (4) The activation parameters for channel II were assumed to be the same for the three isomers, on the assumption that the rearrangement transition

state should be similar for the three isomers. The fit to presently available experiments is not very sensitive to these channel II values, so that small differences between the isomers would not be significant to the present modeling procedure.

With these principles in mind, the modeling parameters for channels I and II were assigned as follows:

Channel I: The kinetic parameters for iodobenzene ion dissociation are $E_0 = 2.38$ eV, $\Delta S^\ddagger = 7.44$ eu. These were the initial values adopted for channel I, which were then adjusted to the extent necessary to fit the available experimental information. The adoption of a ΔS_1^\ddagger value around +7 eu is reinforced by comparison with the dissociation of neutral iodotoluene. As noted by Lifshitz,¹⁷ Arrhenius preexponential factors for equivalent ionic and neutral reactions are about equal. Thermal decomposition of *o*-iodotoluene neutral has been studied in a shock tube at high pressure (2–6 atm).¹⁸ For the simple bond breaking reaction, the rate expression was $k(o\text{-CH}_3\text{C}_6\text{H}_4\text{I} \rightarrow o\text{-CH}_3\text{C}_6\text{H}_4 + \text{I}) = 1.4 \times 10^5 \exp(-33\,346/T) \text{ s}^{-1}$ at 1100 K, corresponding to a ΔS^\ddagger of about 6.16 cal/K at 1100 K.

Channel II: An initial estimate of the channel II parameters can be made from the low-energy photodissociation rate-energy values for *p*-ITOL.³ As indicated by the photoionization experiments of ref 2, this dissociation is dominated by channel II in the 2.5–2.7-eV range. The kinetic parameters assigned from the rate-energy curve in ref 3 were $E_0 = 1.90$ eV, $\Delta S^\ddagger = -4$ eu. Allowing for the small contribution to this curve of channel I dissociations as deduced from the present modeling, these values were adjusted slightly to give the values $E_{0\text{II}} = 1.88$ eV, $\Delta S_{\text{II}}^\ddagger = -7.0$ eu which were used for all three isomers in the present analysis.

Among the extensive experimental data which have been published for these dissociations, we considered the following to be the most valuable for parametrizing and verifying our comprehensive kinetic model:

(1) The PEPICO rate-energy values of Olesik et al.⁶ for *p*-ITOL over the range 3.1–3.7 eV. Their lowest energy curve was fitted as a single exponential, giving a rate constant of $9 \times 10^{-4} \text{ s}^{-1}$. They fitted their other data sets to biexponential functions. We believe their decomposition into slow and fast channels is unconvincing, both because biexponential fits to their data require more confidence in the accuracy of the data than we think is warranted, and especially because it is very hard to find a sensible physical picture of the dissociation which would lead to biexponential decay. (Competing channel I and channel II dissociations lead to a prediction of single-exponential decay of the parent ion.) Recent discussion by the Baer group¹⁹ indicates that they also no longer have confidence in the biexponential analysis of their earlier work. Accordingly we refitted their raw data (their Figure 2) with single exponentials and obtained the rate-energy points plotted on our Figure 3. Interpreted in this way, we consider the data of Olesik et al. and the resulting rate constants, to be worthy of quantitative confidence.

(2) The photodissociation rate constants for thermalized *p*-ITOL reported by Dunbar and Lifshitz³ at 2.0–2.3 eV. This study also assigned the effect of infrared radiative relaxation on the observed parent ion dissociation time constant, which for wavelengths longer than 532 nm was found to give a significant correction to the observed apparent unimolecular dissociation rate constant. The 532-nm rate constant was reconfirmed in the present work.

(3) The branching ratios for channel I and channel II for metastable *p*-ITOL and *m*-ITOL with a range of dissociation time constants from 10 to 120 μs , reported by Lifshitz et al.² from measurements in the cylindrical quadrupole ion trap. These branching ratios were assigned by deconvoluting the bimodal MIKES line shapes. While the experiment was unable to correlate the branching ratios directly with corresponding internal energy

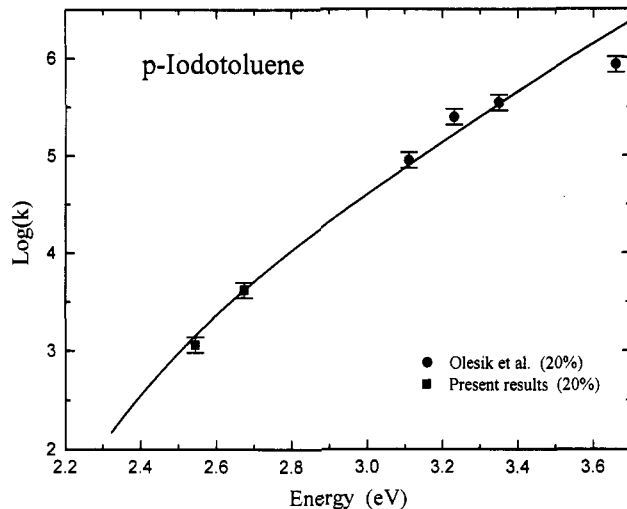


Figure 3. Rate-energy values from the present data and from the results of Olesik et al.⁶ Rather arbitrary error bars of 20% have been assigned to all the points. The solid curve is the modeled rate-energy curve (sum of channels I and II) from the present model.

values, it is possible to make this correspondence once the rate-energy curve has been assigned, and we do this below.

An error in ref 2 should be noted: the energy axis (*x* axis) for Figure 10 of that paper was erroneous. The correct energy values are about 3 times larger. The KERD data shown in this figure, with corrected energy scale, are in good quantitative agreement with the comparable data given by Choe and Kim (Figure 5b of ref 4).

(4) The MIKES line shapes reported by Holmes et al.⁹ These were not analyzed with as much quantitative rigor as the MIKES curves of ref 2 but are in reasonable agreement with the latter and are especially valuable in giving information about *o*-ITOL.

(5) The present photodissociation rate measurements on all three isomers at 2.54 and 2.67 eV. Since the ions were thermalized prior to photoexcitation, the internal energies are well-known and these rate-energy points should be reliable.

(6) The metastable dissociation rate and MIKES line shape for *m*-ITOL reported by Choe and Kim.⁴ They also reported results for photodissociated ions which were potentially valuable to modeling. However, their photodissociation results do not fit quantitatively into the picture built up from the other data sources. We concluded that either our model for *m*-ITOL is fundamentally wrong, or else the photodissociation results of Choe and Kim contained an unrecognized problem. Considering the latter to be more likely, we suggest that the charge-transfer ionization to produce *m*-ITOL in their experiment was more complicated than expected and produced ions of lower internal energy than expected. Accordingly, we have not attempted to fit their photodissociation results into the quantitative model. (See Appendix A for a fuller discussion of these results.)

The present modeling results take the form of rate-energy curves for the two competing dissociation channels available to the ITOL parent ion. The kinetic models for the three isomers are shown in Figures 4–6, and the corresponding RRKM kinetic parameters for the two channels are shown in Table 3. The net, observable dissociation rate is the sum of the two individual rate-energy curves. These summed curves are shown on the three figures and also are collected in Figure 7 for direct comparison. Also included on Figures 4–6 are the dissociation rate points for all three isomers measured in the present study, and the dissociation rates for *p*-ITOL from Olesik et al.⁶ It is clear that the models represent these known rates very well.

The modeled branching ratio for the two channels is obtained directly from the ratio of rate constants at any given energy. Figures 8–10 show the predicted branching ratio plots for the three isomers, along with the measured results of Lifshitz et al.²

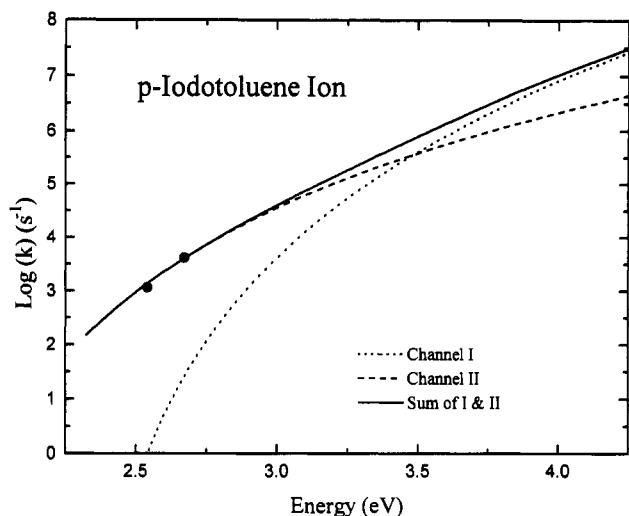


Figure 4. *p*-ITOL dissociation rate constant predictions from the present model for the two channels, and for the sum of the channels. The activation parameters used are listed in Table 3. The two data points are the experimental values from the present work.

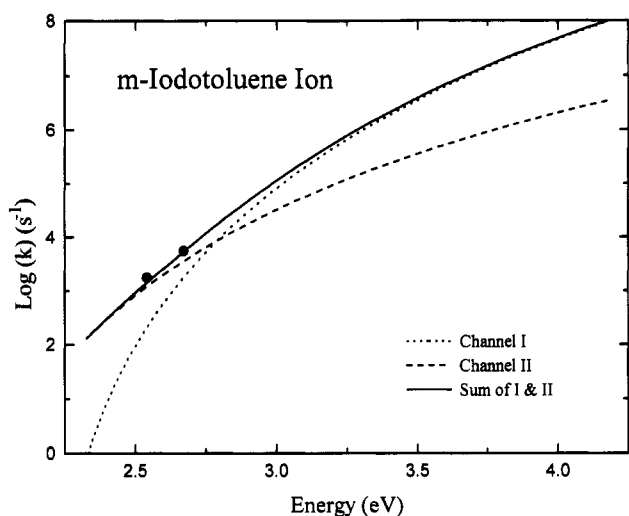


Figure 5. Same as Figure 4, for *m*-ITOL.

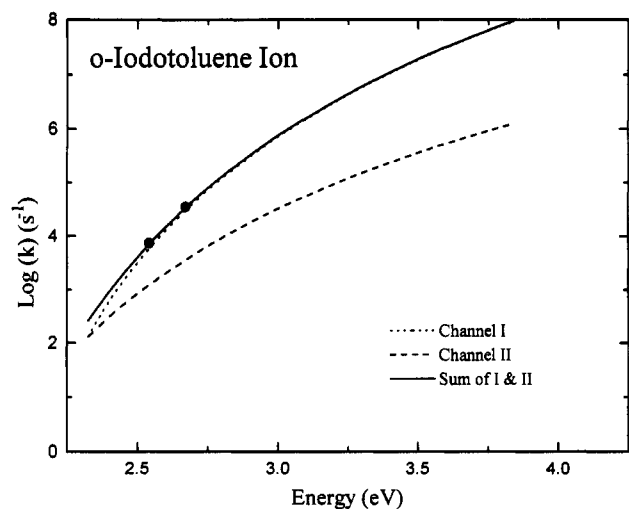


Figure 6. Same as Figure 4, for *o*-ITOL.

for meta and para. It is seen that the measurements of Lifshitz et al. are not quite reproduced within the expected uncertainty. However, the agreement is approximately correct, and in particular the models successfully predict that over the range of measurements channel II is high and nearly constant for *p*-ITOL, while channel I rises rapidly with increasing energy for *m*-ITOL.

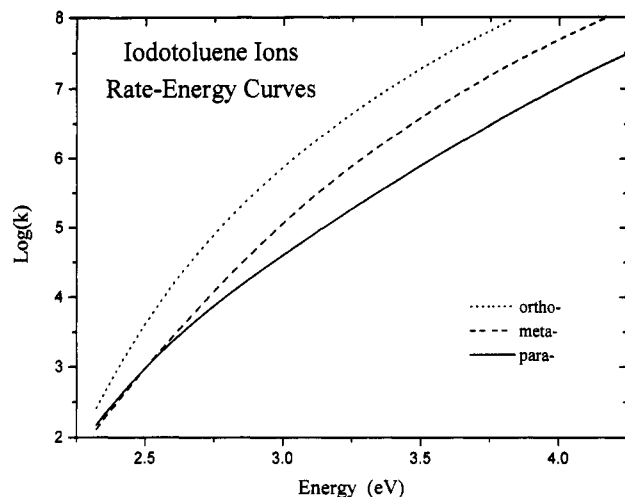


Figure 7. Modeled rate-energy curves for the three ITOL isomers (sum of channels I and II).

TABLE 3: RRKM Kinetic Parameters E_0 (eV) and ΔS^\ddagger (eu)

	<i>p</i> -ITOL	<i>m</i> -ITOL	<i>o</i> -ITOL
E_0^I	2.41	2.24	2.11
E_0^{II}	1.89	1.88	1.88
ΔS^\ddagger_I	7.75	7.44	7.44
ΔS^\ddagger_{II}	-6.98	-7.00	-7.00

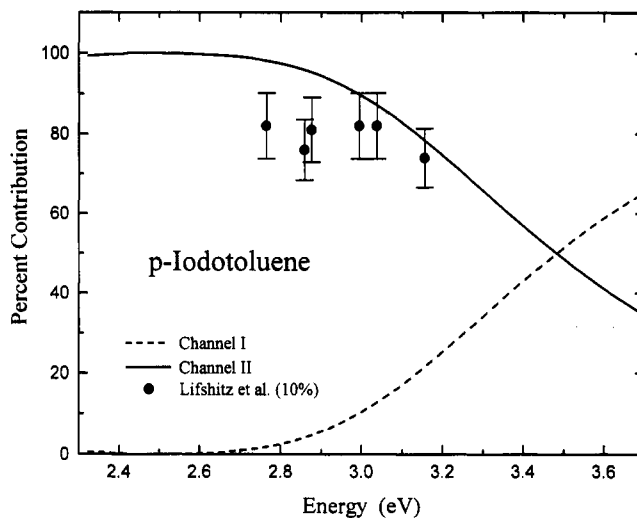


Figure 8. Branching ratios for the two channels for *p*-ITOL, calculated from the present model, assuming that the fraction of the overall dissociation occurring through each channel is proportional to its rate constant, and using activation parameters from Table 3 for the individual channels. The experimental points are from Lifshitz et al.² with the energy scale fixed through modeling as described in the text.

Discussion

The models are reasonably successful in matching the observed behavior of the three isomers. For ions in the metastable region of dissociation rates (10^5 – 10^6 s⁻¹) it is correctly predicted that para will show a mixture of comparable amounts of channel I and channel II dissociations, while for ortho and meta channel I will dominate. It is correctly modeled that in the low-energy region covered by photodissociation rate measurements channel I will dominate for ortho, giving a large rate with a steeply rising rate-energy curve, while for meta and para channel II will predominate, giving lower rates and a flatter rate-energy curve. The quantitative branching ratios of Lifshitz et al.³ are modeled approximately correctly, as is the branching ratio for metastable ions measured by Choe and Kim.⁴ The result from MIKES line shapes⁹ that para has a much higher contribution from channel II than meta and ortho is accounted for.

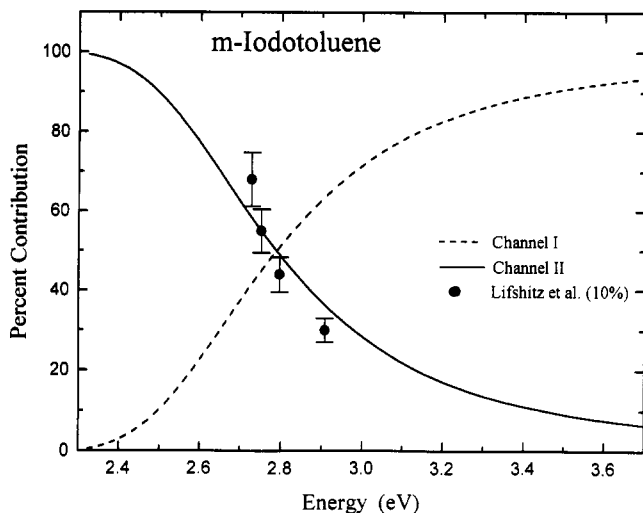


Figure 9. Same as Figure 8, for *m*-ITOL.

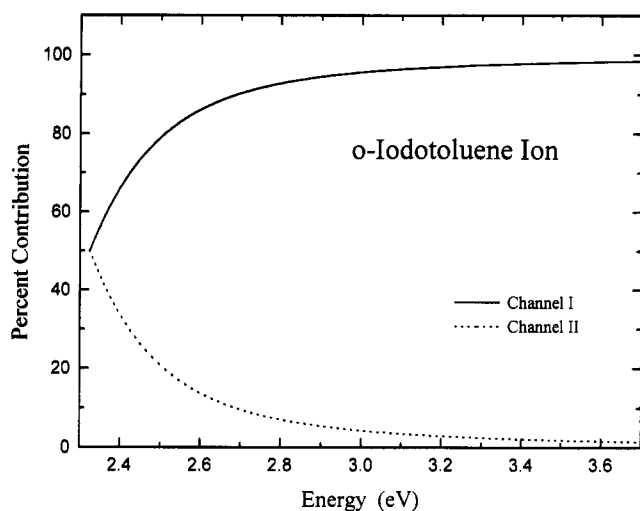


Figure 10. Modeled branching ratio curves as in Figure 8, for *o*-ITOL.

A prominent feature of the present experimental results is that the *o*-ITOL dissociation is much faster (by almost an order of magnitude) than *m*- and *p*-ITOL. The modeling outlined here ascribes this difference to an increase in the channel I rate, reflecting a lower channel I activation energy for the ortho case. The steep energy dependence of the rate, implying a loose transition state, gives a justification of this assumption (as suggested by the excellent fit to the model in Figure 6). Metastable ion MIKES peak shapes also support our assumption that it is channel I, and not channel II, that is exceptionally fast for the ortho case: The MIKES spectra of Holmes et al.⁹ show a mixture of channel I and channel II products for *p*-ITOL, but neither meta nor ortho shows any observable extent of channel II in the MIKES line shapes.⁹ As already discussed, the MIKES results of Holmes et al.⁹ are as expected for para and meta and agree with the predictions of Figures 4 and 5 in the metastable ion region ($\sim 10^6$ s⁻¹). For ortho, their observation of exclusively channel I products agrees with the situation described by Figure 6, confirming that channel I is dominant around 3.0-eV internal energy. This would not be the case if channel II were much faster in the ortho case, so our assignment of a fast channel I reaction in this case is confirmed.

Since channel I is a direct dissociation with a loose transition state, its activation energy E_0 should be close to the thermochemical threshold for formation of tolyl ions. The heats of formation derived from this assumption are shown in Table 4. These agree with the previous results for meta and para shown in Table 2 within the combined uncertainties. However, it is notable that our results suggest that *p*-Tol is slightly more stable

TABLE 4: Gas-Phase Heat of Formation from Present Analysis (kJ mol⁻¹)

ion	$\Delta H_{f,0}$
<i>p</i> -Tol	1083
<i>m</i> -Tol	1091
<i>o</i> -Tol	1080

than *m*-Tol, reversing the order of Table 2. We believe our value is the best available for *o*-Tol.

The complete lack of correspondence between the channel II activation energy and the thermochemistry of the products is very clear. If we naively take the channel II E_0 values given in Table 3 and derive an "apparent" heat of formation for C₇H₇⁺, we obtain 1058 kJ mol⁻¹. As is seen by comparing this with the heats of formation of Bz and Tr in Table 4, this "heat of formation" is about 150 kJ mol⁻¹ too high, which is an enormous discrepancy. There is clearly a large, rate-determining rearrangement barrier in channel II, as suggested qualitatively in Figure 1. This illustrates the severe danger arising from attempts to draw thermochemical conclusions from dissociation threshold measurements for dissociation reactions which are not direct bond cleavages. In this case the existence of a large reverse activation energy for channel II is plainly signalled by the large kinetic energy release observed for this channel.^{3,4,9}

Conclusion

The quantitative two-channel kinetic model formulated here is quite successful in describing these dissociation processes with regard to the dissociation rates, the product mix observed for metastable ion dissociations, and the product mix obtained from dissociative photoionization. The large enhancement observed for the ortho dissociation rate relative to the other two isomers is attributed to a lower activation energy in channel I. Whether the lowering of the activation energy is due to steric interactions, or to other effects, is an interesting question for future consideration.

This modeling is useful in suggesting fruitful areas for future data gathering on these systems. Information on the para system is quite extensive, and our understanding seems reasonably satisfactory. It would be interesting to check the model prediction that channel II products will become dominant above 3.5 eV for this isomer. For meta, confidence in the kinetic model would be increased with PEPICO dissociation rates in the higher-energy regime from 3–4 eV, and it would also be useful to clarify the product branching ratio situation in the region above 3 eV. For the ortho isomer rate data are needed at energies above 2.7 eV, and product branching ratios at all energies. Because data are so sparse, modeling for this isomer is still rather uncertain.

Acknowledgment. The support of the National Science Foundation and of the donors of the Petroleum Research Fund, administered by the American Chemical Society, is gratefully acknowledged.

Appendix

Reanalysis and Discussion of the Fast-Beam Photodissociation Results. For *m*-ITOL, Choe and Kim⁴ reported the unimolecular dissociation rates and the fraction of channel I and channel II (determined by deconvoluting the KER curve) for (1) metastable ions produced by electron impact, and (2) ions produced by charge transfer and photoexcited at 515 and 488 nm. Their rate, their KER curve, and their assignment of the fraction of channel I for the metastable ions are in acceptable agreement with the metastable ion measurements of Lifshitz et al.² and can be accepted with confidence. However, their photodissociation results do not fit into our understanding of this ion, and we suggest that the production of parent ions by CS₂⁺ charge transfer actually

produces a broad distribution of internal energies rather than the monoenergetic ions (with a thermal distribution) assumed in their analysis.

The rate constant measured for the photodissociated ions is implausibly low. The value assigned to ions of 4.4 eV internal energy from this experiment is $3.5 \times 10^7 \text{ s}^{-1}$. Combining this value with the low-energy values from the present work leads inescapably to a very flat rate-energy curve for channel I, and to the assignment of a strongly negative ΔS^\ddagger (as was also concluded by Choe and Kim). We consider this unacceptable for the simple bond cleavage of channel I.

The decomposition of the photoexcitation KER curve to find the fraction of channel I dissociations has two unsatisfactory features: (1) the assigned fraction of channel I for photodissociation products is actually larger than for the lower-energy metastable ions, whereas Lifshitz et al.² clearly showed that this fraction declines with increasing internal energy; (2) the deconvoluted KER curve corresponding to channel II is very different in shape from that obtained from the metastable ion results and has a large and implausible number of ions dissociating with near-zero KER. We have reanalyzed the KER curve of Choe and Kim's Figure 4a, making the assumption that the channel II KER curve has the same shape as the channel II KER curve for metastable ions; this reanalysis indicates about 23% of channel I for the photodissociated ions. This is more satisfactory, being smaller than the metastable-ion value of 36%, but as can be seen from Figure 9, 23% is still a much higher percent of channel I than is expected from our kinetic model at 4.4-eV internal energy.

Taking together the two features that the rate at their nominal 4.4-eV energy is too low, and the fraction of channel I is too high, we infer that the actual average energy of the dissociating ions in Choe and Kim's experiment was probably lower than 4.4 eV, in fact probably near 4.0 eV. This energy deficit of about 0.4

eV does not seem implausible for charge-transfer ionization of a large molecule by a polyatomic reagent ion.

References and Notes

- (1) Pratt, S. T.; Chupka, W. A. *Chem. Phys.* **1981**, *62*, 153. Dannacher, J.; Rosenstock, H. M.; Buff, R.; Parr, A. C.; Stockbauer, R. L.; Bombach, R.; Stadelmann, J.-P. *Chem. Phys.* **1983**, *75*, 23. Dunbar, R. C.; Honovich, J. P. *Int. J. Mass Spectrom. Ion Proc.* **1984**, *58*, 25. Dunbar, R. C. *Chem. Phys. Lett.* **1985**, *115*, 349.
- (2) Lifshitz, C.; Levin, I.; Kababia, S.; Dunbar, R. C. *J. Phys. Chem.* **1991**, *95*, 1667.
- (3) Dunbar, R. C.; Lifshitz, C. *J. Chem. Phys.* **1991**, *94*, 3542.
- (4) Choe, J. C.; Kim, M. S. *Int. J. Mass Spectrom. Ion Proc.* **1991**, *107*, 103.
- (5) Traeger, J. C.; Kompe, B. M. *Int. J. Mass Spectrom. Ion Proc.* **1990**, *101*, 111.
- (6) Olesik, S.; Baer, T.; Morrow, J. C.; Ridal, J. J.; Buschek, J.; Holmes, J. L. *Org. Mass Spectrom.* **1989**, *24*, 1008.
- (7) Dunbar, R. C.; Honovich, J. P.; Asamoto, B. *J. Phys. Chem.* **1988**, *92*, 1733.
- (8) Stapleton, B. J.; Bowen, R. D.; Williams, D. H. *J. Chem. Soc., Perkin Trans. 2* **1979**, 1219.
- (9) Holmes, J. L.; Blair, A. S.; Weese, G. M.; Osborne, A. D.; Terlouw, J. K. *Adv. Mass Spectrom.* **1978**, *7*, 1227.
- (10) Robinson, P. J.; Holbrook, K. A. *Unimolecular Reactions*; Wiley-Interscience: New York, 1972. Forst, W. *Theory of Unimolecular Reactions*; Academic Press: New York, 1973.
- (11) Dunbar, R. C. *J. Phys. Chem.* **1987**, *91*, 2901.
- (12) See, for instance: Baer, T. *Adv. Chem. Phys.* **1986**, *64*, 111.
- (13) Dunbar, R. C. *J. Chem. Phys.* **1989**, *91*, 6080.
- (14) Baer, T.; Morrow, J. C.; Shao, J. D.; Olesik, S. *J. Am. Chem. Soc.* **1988**, *110*, 5633.
- (15) Klots, C. E. *J. Phys. Chem.* **1992**, *96*, 1733.
- (16) Lias, S. G.; Bartmess, J. E.; Liebman, J. F.; Holmes, J. L.; Levin, R. D.; Mallard, W. G. *J. Phys. Chem. Ref. Data* **1988**, *17*, Suppl. 1.
- (17) Lifshitz, C. *Adv. Mass Spectrom.* **1989**, *11*, 713.
- (18) Robaugh, D.; Tsang, W. *J. Phys. Chem.* **1986**, *90*, 5363.
- (19) Booze, J. A.; Schweinsburg, M.; Baer, T. *J. Chem. Phys.* **1993**, *99*, 4441.